

Spatiotemporal Source Apportionment of Ozone Pollution over the Greater Bay Area

Yiang Chen ¹, Xingcheng Lu ^{2*} Jimmy C.H. Fung ^{1,3}

¹ Division of Environment and Sustainability, The Hong Kong University of Science and Technology, Clear Water Bay, Kowloon, Hong Kong SAR, China

² Department of Geography and Resource Management, The Chinese University of Hong Kong, Sha Tin, New Territory, Hong Kong SAR, China

³ Department of Mathematics, The Hong Kong University of Science and Technology, Clear Water Bay, Kowloon, Hong Kong SAR, China

Correspondence to: Xingcheng Lu (xingchenglu2011@gmail.com)

Abstract. It has been found that ozone (O₃) pollution episodic cases ~~are~~ prone to appear when the Greater Bay Area (GBA) is under the control of typhoons and sub-tropical high-pressure systems in summer. To prevent these pollutions effectively and efficiently, it's essential to understand the contribution of O₃ precursors emitted from different periods and areas under these unfavorable weather conditions. In this study, we further extended the Ozone Source Apportionment Technology (OSAT) from the Comprehensive Air Quality Model with Extensions (CAMx) model to include the function ~~of~~ tracking the emission periods of O₃ precursors. ~~Subsequently, then~~ the updated OSAT module was applied to investigate the spatial-temporal contribution of precursors emissions to the O₃ concentration over the GBA in July and August 2016, when several O₃ episodic cases appeared in this period. Overall, the emissions within ~~the~~ GBA, from other regions of Guangdong province (GDo), and the neighbouring provinces ~~were~~ the three major contributors, ~~which~~ accounting for 23%, 15%, and 17% of ~~the~~ monthly average O₃ concentration, respectively. More than 70% of O₃ in the current day ~~was~~ mainly formed from the pollutants emitted within 3 days and the same day's emission contributed approximately 30%. During the O₃ episodes, when ~~the~~ typhoon approached, more pollutants emitted 2-3 days ago from the GDo and adjacent provinces were transported to the GBA, leading to ~~an~~ the-increase ~~in~~ O₃ concentrations ~~in~~ within this region. Under the persistent influence of northerly wind, the pollutants originating from eastern China earlier than 2 days ago can also show ~~an~~ noticeable/obvious impact on the O₃ over the GBA in the present day, accounting for approximately 12%. On the other hand, the O₃ pollution ~~was~~ primarily attributed to the local emission within 2 days when the GBA ~~was~~ mainly under the influence of the sub-tropical high-pressure systems. These results indicated ~~ed~~ the necessity to consider the influence of meteorological conditions in implementing the control measures. Meanwhile, analogous relationships between source area/time and receptor were derived by the zero-out method, supporting the validity of the updated OSAT module. Our approach and findings could offer more spatial-temporal information about the sources of O₃ pollutions, which could aid in the development of effective and timely control policies.

1. Introduction

As one of the major air pollutants, ozone (O₃) is a secondary pollutant formed by the photochemical reactions of nitrogen oxides (NO_x) and volatile organic compounds (VOCs) in the presence of solar radiation. ~~The~~ Surface O₃ has detrimental effects on human health, such as causing respiratory and cardiovascular problems (Maji et al., 2019; Yin et al., 2017). It could also lead to the reduction of crop yield and the damage of vegetation (Gong et al., 2021; Wang et al., 2022c). With the implement~~ation~~ing of a series of control policies in China since 2013, the concentrations of other air pollutants, including particulate matter with aerodynamic diameters less than 2.5µm (PM_{2.5}), NO_x, and sulfur dioxide (SO₂), have gradually decreased. In contrast, due to the large reduction of NO_x emission and ~~limited~~less control of VOCs emission in the early stage of the control period (Liu et al., 2023), the O₃ concentration still continuously increased and has become the ~~primary~~major air pollutant across China. The Greater Bay Area (GBA), including nine cities in the Pearl River Delta (PRD) region, Hong Kong (HK), and Macau Special Administrative Regions (SAR), is one of the most developed agglomerations in China and also

48 ~~faces~~ ~~facings~~ with the heavy O₃ pollution problem. Based on the analysis of surface monitor observation, Cao et al.
49 (2024) and Feng et al. (2023) ~~revealed an overall upward trend in the maximum daily 8-h average (MDA8) O₃ in~~
50 ~~the PRD region and HK, with an increase of 1.11 and 0.22 ppbv/year from 2013 to 2019 and from 2011 to 2022,~~
51 ~~respectively, found that the daily maximum 8hr average (MDA8 O₃) in the PRD region and HK showed an overall~~
52 ~~upward trend by 1.11 and 0.22 ppbv/year from 2013 to 2019 and from 2011 to 2022, respectively.~~

Formatted: Subscript

53 The formation of O₃ is closely related to the sources of its precursors, and much effort has been devoted to
54 investigating the source region and source category of O₃ in the GBA using different methods (Liu et al., 2020a).
55 He et al. (2019) applied the positive matrix factorization (PMF) method to resolve the anthropogenic sources of
56 VOCs. Combining ~~with~~ a photochemical box model with the master chemical mechanism (PBM-MCM), they
57 found that vehicular was the most significant source ~~of to~~ the O₃ formation, followed by biomass burning and
58 solvent usage. Li et al. (2012) applied the CAMx-OSAT numerical model to track the source contribution to O₃
59 in the GBA region and found that elevated local and regional contributions ~~wereis~~ dominant ~~duringunder~~ the O₃
60 episodes. Yang et al. (2019b) applied the NAQPMS model with an on-line source apportionment module to
61 explore the sources of O₃ in different seasons in the PRD region. Their results show~~eds~~ that the mobile ~~wasis~~ the
62 largest contributor, followed by industry. Fang et al. (2021) used multi-modelling source apportionments to
63 quantify the source impact on O₃ in the PRD region. The on-road mobile and industrial process were found ~~to~~
64 ~~beas~~ two major contribution ~~sectorsseetions~~. Integrating satellite data and sensitivity model simulations, Wang et
65 al. (2022a) found that enhanced biogenic emission and cross-regional transport ~~due toby~~ approaching typhoons
66 ~~are were~~ significant factors ~~leading to the~~ ozone pollution in the PRD and Yangtze River~~l~~ Delta (YRD) regions.
67 In addition to the source region and category, ~~the~~ emitting time of pollutants is also an important perspective that
68 needs ~~a better understanding to be better understood~~ for effective and efficient control policymaking. ~~Several~~ ~~Some~~
69 studies have attempted to evaluate this temporal perspective (Xie et al., 2021; Ying et al., 2021). Xie et al. (2023)
70 analysed the age evolution of PM_{2.5} during a haze event in eastern China. It showed that during the regional
71 transport stage, more aged particles from the North China Plain (NCP) were transported to the downwind YRD
72 region ~~and~~, leading to a sharp increase in the average age of different components of PM_{2.5} in ~~the~~ YRD. Chen et
73 al. (2022c) ~~investigatedanalyses~~ the temporal contributions of emissions to the concentration of PM_{2.5} in the PRD
74 region and found that pollutants emitted ~~from~~ 2 days earlier were trapped within the PRD region due to the weak
75 wind during the episodic pollution. However, these studies mainly focused~~ed~~ on the PM_{2.5} and the temporal
76 contribution of sources to the O₃ in the GBA region still remain~~s~~ unclear.

77 ~~In addition to~~ ~~Besides~~ emission, ~~the~~ meteorological conditions, another key factor that can affect the transportation,
78 production, and destruction of O₃ and its precursors, ~~have~~ also received much attention and ~~have~~ been extensively
79 studied (Lu et al., 2019; Wang et al., 2017; 2022b). The long/short-term effects of ~~changes in meteorological~~
80 ~~conditions meteorological changes~~ on ozone concentrations have been investigated through ~~various a variety of~~
81 methods, such as statistical analysis of observations and numerical modelling (Yang et al., 2019a; Xu et al., 2023a;
82 Zheng et al., 2023). Liu and Wang (2020b) conducted sensitivity simulations by the CMAQ model to evaluate the
83 contribution of ~~variations in~~ weather conditions ~~variation~~ to summer O₃ levels from 2013-2017. Their results
84 show~~ed~~ that the meteorological conditions were more conducive to ozone formation from 2014 to 2016 than in
85 2013, ~~and it can leading~~ to an increase of more than 10 ppbv in MDA8 O₃ in Guangzhou. Different objective and
86 subjective classification technologies have been applied to summarize the impacts of unfavorable weather patterns
87 on O₃ pollution (Han et al., 2020; Chen et al., 2022b; Cao et al., 2023). Gao et al. (2018) summarized the
88 common~~ly~~ synoptic patterns in the Guangdong province that O₃ pollution always occurred and concluded that the
89 sub-tropical high-pressure system and typhoons are two major patterns accounting for more than 60% ~~of cases~~ in
90 the PRD regions during 2014 – 2016. The major influenc~~ing~~ ~~ing~~ factors and the dominant ~~e~~ ~~contributed~~ physical and
91 chemical processes were also identified and analyzed (Gong et al., 2022; Zeren et al., 2022; Wu et al., 2023).
92 Ouyang et al. (2022) analysed the impact of a subtropical high and a typhoon on ozone pollution in the PRD
93 region and found that low relative humidity, high boundary layer height, weak northerly surface wind, and strong
94 downdrafts were the main meteorological factors contributing to the pollution. Deng et al. (2019) illustrated that
95 the actinic flux ~~was is~~ the important cause of the co-occurrence of high ozone and aerosol pollution under the
96 control of typhoon periphery. Li et al. (2022) also investigated the impact of peripheral circulation characteristics
97 of typhoons and found that the chemical formation and vertical mixing effects ~~are were~~ two major contributors to
98 the enhancement of O₃ levels, while the advection showed negative values. Qu et al. (2021) analysed the typhoon-
99 induced and non-typhoon O₃ events in the PRD region and revealed that under the influence of typhoons, the
100 contributions from the transport processes and sources outside the PRD increased. Usually, the ozone events are
101 attributed to changes in meteorological conditions rather than sudden increases in emission intensity (Lin et al.,
102 2019; Xu et al., 2023b). The changes ~~in ef~~ weather conditions will affect the time-sensitivity of emitted pollutants

103 and lead to different types of O₃ pollution, ~~that can result from such as~~ long-range transport of ~~aged~~ pollutants
104 or accumulation of local fresh pollutants. Hence, it ~~is~~ of great importance to clarify the impact of the pollutants
105 from different source areas and emitting periods on the O₃ pollution under different weather conditions in the
106 GBA.

107 In this study, the CAMx-OSAT model was extended and used to track the temporal contribution of pollutants to
108 the O₃ pollutions over the GBA under the impact of typhoons and sub-tropical high pressure during July and
109 August in 2016, the two most important weather systems that influence O₃ pollutions over the GBA. The rest of
110 this paper is organized as follows. The temporal source apportionment (TSA) method, the configuration of
111 experiments, and the ozone episodes ~~are~~ introduced in section 2. The spatial-temporal source apportionment
112 results and zero-out simulation results ~~are~~ shown and discussed in section 3. The major conclusions ~~are~~
113 summarised in section 4.

114

115 2. Methodology and Data

116 2.1 Temporal Source Apportionment Method

117 Previously, we have successfully implemented the PM_{2.5} temporal source apportionment (TSA) method in the
118 Comprehensive Air Quality Model with Extensions (CAMx) model and applied it to investigate the temporal
119 influence of emissions on PM_{2.5} in the GBA (Chen et al., 2022c). Here, we further extend this method to track the
120 temporal contribution of emissions to the precursors and the formation of O₃ and its precursors. Similar to the
121 OSAT method, the input data used in the TSA method developed in this work include the source area map and
122 hourly emission data. The source area map assigns each model grid cell to one of the specific source regions. The
123 hourly emission data is the same as the one used in the normal CAMx model simulation without turning on the
124 source apportionment module. The basic mechanism of the TSA method is to track the contribution of pollutants
125 from different emitting periods using a set of tracers. In the TSA method (Fig. 1), the Precursor Tracer Day-*x*
126 was used to track the precursors emitted from *x* days ago. The O₃ Tracer Day-*x* was used to track the O₃ formed from
127 the precursors emitted from corresponding *x* days ago (namely Precursor Tracer Day-*x*). The tracers in Day-*x*
128 can be set into different finer periods (e.g., every 1 hour, 6 hours, 24 hours) as required. The total number of tracers
129 ~~number~~ will be decided according to the ~~entire~~ tracking period and the minimum tracking period per tracer.
130 For instance, if the ~~entire~~ tracking period is 5 days and the minimum tracking period per tracer is every 6
131 hours, the total number of tracers ~~number~~ will be 20. In each time step, the tracers go through all the processes,
132 including emission, transport, diffusion, and chemical reactions, sequentially, as in the normal CAMx model
133 simulation. Therefore, the precursors and O₃ tracers that tracked different periods are calculated simultaneously.
134 When the pollutants emitted from the sources, they will be assigned to the Precursor Tracer in Day-0, while the
135 Precursor Tracers that tracked other periods and the O₃ Tracers remain unchanged. The data transfer between
136 tracers (e.g., Day-1 to Day-2, and Day-0 to Day-1, dash arrow in Figure 1) will be conducted once after one day's
137 simulation. As shown in the Figure 1, during each day's simulation, the contribution of the present day's emission
138 is consistently ~~will always be~~ tracked by the Day-0 tracers. After completing the current day's simulation and
139 before starting the next day's simulation, each tracer Day-*x*'s value transfers to the corresponding tracer Day-
140 (*x*+1), which represents one day earlier than Day-*x*, following the specified sequence in the following sequence.
141 For example, beginning from the penultimate tracer, namely values in Day-3 transfer and add into Day-4, then the
142 values in Day-2 transfer to Day-3, followed by Day-1 to Day-2, and lastly Day-0 to Day-1 (Dash arrow in Figure
143 1). Here, the value in Day-3 tracer will be added into the last tracer (Day-4) because the last tracer represents the
144 total contribution of pollutants emitted earlier than 3 days ago. Same as the OSAT method, the TSA method also
145 utilizes the photochemical indicator, namely, the ratio of the production rate of hydrogen peroxide (H₂O₂) and
146 nitric acid (HNO₃), to determine the sensitivity of O₃ formation. When the O₃ formation is classified as NO_x-
147 limited (VOC-limited), the contributions are distributed to the NO_x (VOCs) sources emitted at different periods,
148 based on the proportion of their emissions to the total NO_x (VOCs) emissions. More details of this method can
149 be found in Chen et al. (2022c).

Formatted: Font: Not Italic

Formatted: Font: Not Italic

Formatted: Font: Not Italic

Formatted: Font: Not Italic

Formatted: Font: Not Italic

Formatted: Font: Not Italic

Formatted: Font: Not Italic

Formatted: Font: Not Italic

Formatted: Font: Not Italic

Formatted: Font: Not Italic

Formatted: Font: Not Italic

Formatted: Font: Italic

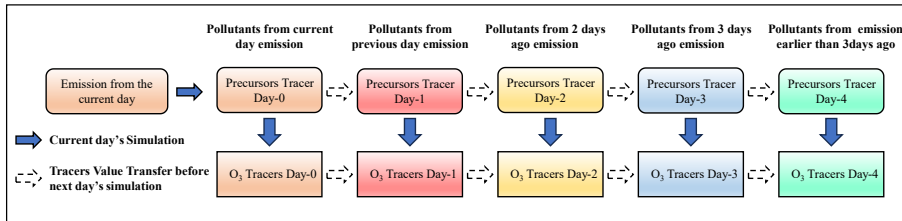
Formatted: Font: Not Italic

Formatted: Font: Not Italic

Formatted: Font: 10 pt

Formatted: Font: Not Italic

Formatted: Font: Not Italic



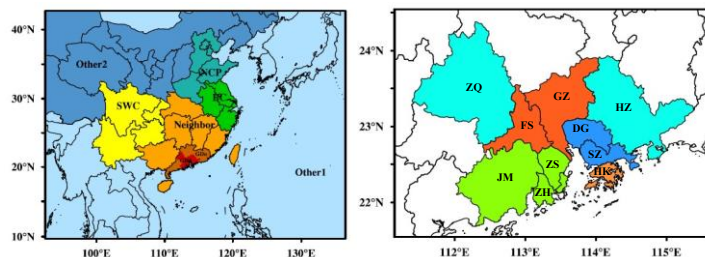
150
151 Figure 1. Schematic diagram of temporal source apportionment (colors represent the pollutants released or formed
152 by emissions on different days).
153

154 2.2 Model Configuration and Evaluation

155 The Weather Research and Forecasting (WRFv3.9) model was applied for meteorological field simulation. The
156 initial and boundary condition for the WRF model was gained from the Final Operational Global Analysis data
157 (FNL). The CAMx v7.1 was used to simulate the spatial-temporal variation of air pollutants. The initial and
158 boundary condition for the CAMx model was provided by the Model for Ozone and Related chemical Tracers,
159 version 4 (MOZART-4). Regarding the emission, a highly resolved emission inventory provided by the Hong
160 Kong Environmental Protection Department (HKEPD) was used for the GBA region, and the Multi-resolution
161 Emission Inventory for China (MEIC, Li et al., 2017) developed by the Tsinghua University was applied for the
162 area outside the GBA region. The biogenic emission for the entire domain was calculated by the Model of
163 Emissions of Gases and Aerosols from Nature (MEGAN version 3.1). The CB05 gas phase chemistry, the
164 ISORROPIA inorganic aerosol scheme, and the SOAP secondary organic aerosol scheme were used in the
165 simulation. This model system has been applied to analyse the source of O₃, NO_x and PM_{2.5} in the GBA region in
166 the previous studies (Lu et al., 2016; Chen et al., 2022a; Chen et al., 2022c). More configuration of this model
167 system can refer to the work of Lu et al. (2016).

168 The three-nested simulation domain of the WRF-CAMx model was shown in Figure S1. The resolution of three
169 domains was 27km, 9km, and 3km, respectively. For the source apportionment experiments, the simulation
170 domain was divided into 12 source regions as shown in Figure 2, including North China Plain (NCP), eastern
171 China (EC), southern western China (SWC), other regions of inland China (Other 2), ocean and other countries
172 (Other 1), neighbouring provinces around Guangdong province (Neighbor), Other region within Guangdong
173 province but outside the GBA (GDo), different sub-regions within the GBA: Guangzhou and Foshan (GF),
174 Shenzhen and Dongguan (SD), Hong Kong (HK), Zhuhai, Zhongshan and Jiangmen (ZZJ), Zhaoqing and
175 Huizhou (GBAo). ~~The cities within the GBA were separated into different sub-regions mainly based on their
176 geographical location, same as the work of Chen et al. (2022e). Since the source contribution to the O₃ in Zhaoqing
177 and Huizhou is relatively different with that of their neighboring cities (Chen et al., 2022a), these two cities were
178 grouped into one sub-region. The cities within the GBA were separated into different sub-regions mainly based
179 on administrated boundaries and their geographical location, same as the work of Chen et al. (2022c). The sub-
180 regions mainly consist of neighboring cities. Zhaoqing and Huizhou, located at the northwestern and northeastern
181 corners, respectively, were categorized into one group since they have a relatively lower emission density than
182 other cities. Previous studies indicated that the air pollutants in Hong Kong were usually more influenced by long-
183 range transport from regions outside the GBA, in contrast to the other cities in the GBA (Li et al., 2012; Chen et
184 al., 2022a; Chen et al., 2022c). Hence, Hong Kong city is treated as a separate entity.~~ The contribution of initial
185 and D1 boundary conditions were also treated as two sources. In the following analysis, for the O₃ concentrations
186 in the target area over the GBA, the influence of pollutants emitted within the target area is treated as the local
187 contribution, and the influence of pollutants originating from the other areas within the GBA region is treated as
188 the regional contribution. The source tracking time period is 5 days. (Day-0, Day-1, Day-2, Day-3 represent the
189 pollutants emitted within the present day, the previous day, two days ago, and three days ago, respectively. Day-4
190 represents the total contribution of pollutants emitted earlier than three days ago). The simulation period is July
191 and August 2016, and the model was spin-up for 7 days to reduce the influence of initial condition.

Formatted: Font: Not Italic



192
193 Figure 2. The configuration of source areas in the source apportionment experiments (One color represents one
194 source area. The GBA source were divided into five source areas. *Other 1* represents ocean and other countries.
195 *Other 2* represents other area within the mainland China in the simulation domain.)

196 The performance of simulated hourly 2-m temperature, 10-m wind speed, and O₃ concentration were evaluated
197 and shown in Table S1. Here, the statistical metrics, including mean bias (MB), normalized mean bias (NMB),
198 index of agreement (IOA), and root mean square error (RMSE), were used for model performance evaluation.
199 The mathematical formulas for these metrics can be found in Table S6. The recommended values suggested by
200 Emery et al. (2001) and EPA (2007) were used as benchmarks and shown in the brackets in Table S1. The
201 temperature ~~is~~was a little overestimated with a ~~mean-bias-(MB)~~ mean bias (MB) of 0.33, while the wind speed ~~is~~was
202 underestimated with a MB of -0.45. The ~~index-of-agreement-(IOA)~~ index of agreement (IOA) ~~is~~was 0.82 and 0.70 for temperature and wind
203 speed, respectively. The MBs and IOAs both fulfilled the criteria. But the ~~root-mean-square-error-(RMSE)~~ root mean square error (RMSE) shows
204 a little higher than the value of criteria. Regarding the O₃, the IOA reaches 0.81. The small positive MB indicates
205 that the model slightly ~~overestimates/overestimated~~ overestimates the O₃ concentration. The ~~normalized-mean-bias-(NMB)~~ normalized mean bias (NMB) is
206 0.13, which also meets the criteria. The time series comparison (Fig. S2) of average O₃ concentration in
207 Guangzhou, Hong Kong and Zhuhai illustrates that the model can well catch and reproduce the variation trend of
208 O₃ concentration in GBA, although there ~~is~~are a few differences between the simulated and measured
209 concentration for some peaks, like the period between 25 July and 31 July in Guangzhou. Overall, the performance
210 of model simulation is comparable to the other studies in this region (Li et al. 2022; Yang and Zhao, 2023).
211 Therefore, the simulation result is reasonable and can be further used for source analysis.

212 2.3 Ozone Episodes

213 There were several O₃ episodes ~~that~~ occurred during the simulation period. Here, the 8-h maximum ~~daily 8-h~~
214 ~~average (MDA8)~~ average (MDA8) O₃ concentration (MDA8) over the GBA was calculated using the observation data from the
215 surface monitors stations (Fig. 3). The O₃ observations were obtained from the China National Environmental
216 Monitoring Centre (CNEMC) and the HKEPD. Here, ~~pollution days were identified when the average MDA8 O₃~~
217 ~~observations concentrations over the GBA exceeded 80ppb (Wang et al., 2022d).~~ To better capture the evolution
218 of the O₃ pollution, based on the characteristics of concentration variation, the days preceding and following the
219 O₃ pollution days were also included in the analysis and the whole period was considered as an O₃ episode. The
220 first O₃ pollution occurred between the 7th and 10th of July (Ep1). During this period, the GBA region was
221 ~~initially/firstly~~ controlled by the sub-tropical high-pressure system. When the typhoon north-westerly moved from
222 the east sea area of the Philippines to ~~wards~~ Taiwan province, the GBA was located in the peripheral subsidence
223 region. After the typhoon made landfall, the high-pressure situation in the GBA was relieved and the O₃
224 concentration decreased. There were another two O₃ episodes between 24 July and 1st August. The GBA was
225 mainly influenced by the sub-tropical high-pressure system during 24th-26th July (Ep 2), while the synoptic
226 condition of ~~the~~ GBA between 30th July-1st August (Ep3) was similar to that of Ep1. During the Ep3 period, ~~there~~
227 ~~was~~ another typhoon moving north-westerly from the east sea area of the Philippines and influencing the
228 GBA region. It was found that this type of typhoon movement path was often accompanied by the occurrences of
229 O₃ pollution in the GBA (Wang et al., 2022a). In late August, under the joint influence of the subtropical high-
230 pressure system and the typhoon, the O₃ over the GBA maintained a high concentration level between the 21st -
231 31st of August (Ep4). Unlike ~~the moving paths of the~~ previous two typhoons, this typhoon ~~moved/was moving~~
232 southerly from the sea areas south of Japan and stayed near the sea areas east of Taiwan province. The typhoon
233 moved north ~~wards~~ after 27th August, and northerly winds prevailed in the GBA. Hence, we conducted the
234 simulation of O₃ concentration in the GBA during July-August 2016 and analysed the spatiotemporal contributions
235 of emissions in these episodic cases.

Formatted: Font: Not Italic

Formatted: Font: Not Italic

Formatted: Font: Not Italic

Formatted: Font: Not Italic

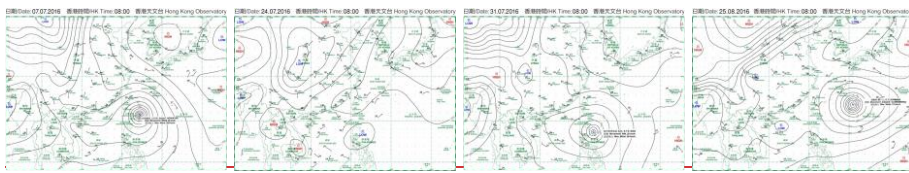
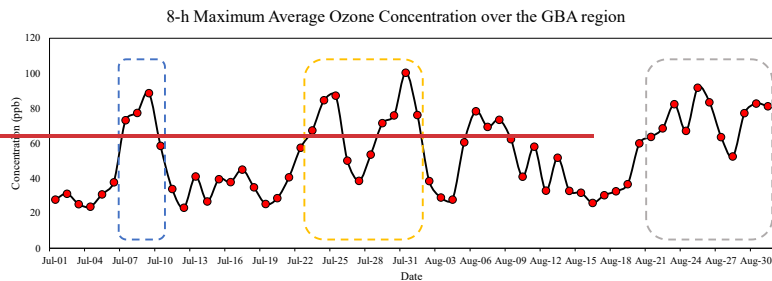
Formatted: Font: Not Italic

Formatted: Font: Not Italic

Formatted: Font: Not Italic

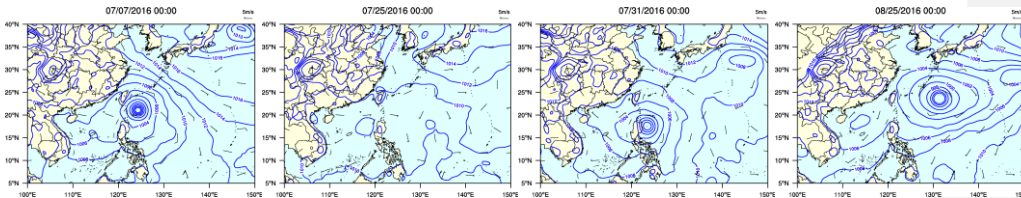
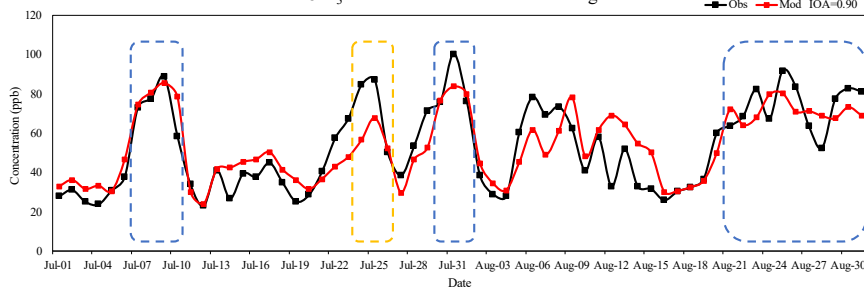
Formatted: Font: Not Italic

Formatted: Justified



236

MDA8 O₃ Concentration over the GBA region



237

Figure 3. The time-series of the MDA8 O₃ concentration over the GBA during July-August 2016 and the synoptic patterns during the O₃ episodes. (The weather charts were downloaded from the Hong Kong Observatory; <https://www.hko.gov.hk/en/wxinfo/currwx/wxcht.htm>)

238

239

240

241

242

243

244

Figure 3. The time-series of the observed and simulated MDA8 O₃ concentration over the GBA during July-August 2016 and the synoptic patterns during the O₃ episodes. (Blue box: typhoon case; Yellow box: sub-tropical high-pressure case. The O₃ observations were obtained from the CNEMC and the HKEPD. The synoptic patterns were plotted using the ERA5 reanalysis data)

245

246

247

248

249

Formatted: Font: Not Bold

Formatted: English (Hong Kong SAR)

3. Result and Discussion

3.1 Source Area Contributions

The contribution of different source areas to the average hourly O₃ concentration average-O₃ in the GBA region was-is shown in Table 1. Here, the contribution from initial and boundary conditions were treated as background

250 contribution. Regarding the monthly average O₃ concentration over the GBA region, the emission within the GBA
251 can contribute about 23%. The pollutants from other regions within Guangdong Province (GDo) and
252 neighbouring provinces also ~~had~~ have large contribution, accounting for approximately 15% and 17%, respectively.
253 Under the influence of prevailing south winds in the summertime, the contribution from ocean and other countries
254 can also account for about 20%. As some studies suggested that O₃ originating from foreign countries is quite
255 limited (Sahu et al., 2021), the main contributor of this source is likely to be marine ship emissions from ocean.
256 The pollutants from other source regions ~~had~~ have limited effect on the O₃ in the GBA.

257 The monthly average source area contribution to four sub-regions within the GBA region can be found in Table
258 S2. Results show that the local emission ~~has had a significant~~ large influence on O₃ in ~~the~~ GF and SD regions,
259 accounting for 17% of O₃ but its ~~has~~ impact was lower than 10% on O₃ in ~~the~~ ZZJ region and HK city. The
260 contribution of GBA regional emissions (contributed by other GBA tagged regions) ~~had~~ a relatively larger impact
261 ~~on~~ the monthly average O₃ concentration in ~~the~~ GF region than the other sub-regions. It's because ~~of~~ the
262 prevailing southerly wind in summer, ~~which resulted in~~ a greater influence of the pollutants within the GBA
263 region ~~have a large influence~~ on O₃ in ~~the~~ GF area. The influences of pollutants from GDo and neighboring
264 provinces ~~on~~ different subregions ranged from 25% to 31%. As ~~the~~ coastal regions, the ZZJ region and HK city
265 were also ~~suffer~~ more affected ~~by~~ from sources of ocean and other countries, which occupied about 24% and 27%,
266 respectively.

267 Regarding the average hourly O₃ concentration over the GBA region in different episode periods, it can be found
268 that, during the typhoon episodes (i.e., Ep1, Ep3 and Ep4), the contribution of non-local emission has increased.
269 The typhoon paths ~~were~~ quite similar in the Ep1 and Ep3 episodes (Fig. S3). Results show that the total
270 contribution of GDo and neighbouring provinces have increased and reached more than 50% for O₃ over the GBA
271 in these two typhoon episodes. As shown in Figure S4, with the approaching of ~~the~~ typhoon, the wind speed
272 increased and the average wind direction over the GBA changed from south to north. Therefore, more pollutants
273 from the surrounding provinces were transported to ~~the~~ GBA. Considering the typical circulation ~~patterns of~~ the
274 typhoon periphery (Figure. S4 and S6), it ~~is inferred~~ was ~~judged~~ that more pollutants may come from Jiangxi,
275 Fujian, and Hunan provinces. During the Ep1 and Ep3 episodes, the contribution of local emission in different
276 sub-regions slightly decreased. With the change of the wind direction from south to north in these two periods,
277 the influence of pollutants within ~~the~~ GBA to O₃ in ~~the~~ GF area decreased from 15% to 8%. The contribution of
278 ~~the~~ GBA emission to the O₃ in other sub-regions increased, especially the ZZJ area and HK city. It is because
279 ~~of~~ with the change of wind direction, these two regions were located at the downwind area of the GF and SD
280 regions, which are the emission hotspots within the GBA. At the same time, the contribution of source from ocean
281 and other countries also decreased ~~by~~ approximately 10%. ~~The influence of GDo and neighbouring provinces~~
282 ~~increased 27%, 21%, 32% and 22% for GF, SD, ZZJ regions and HK city, respectively. The contribution of~~
283 ~~emission from the GDo and neighboring provinces to O₃ concentration in GF, SD, ZZJ regions, and HK city~~
284 ~~increased by 27%, 21%, 32%, and 22%, respectively.~~

285 In another typhoon process (Ep4), where the typhoon's moving path differed from the other two typhoon cases,
286 ~~there was an increase in contribution from GDo and neighbouring provinces under the influence of persistent~~
287 ~~northerly wind an increase in the contribution from GDo and neighbouring provinces was observed due to the~~
288 ~~persistent northerly winds~~. Furthermore, it was observed that pollutants from eastern China (EC) and North China
289 Plain (NCP) could also influence the O₃ levels in the GBA, accounting for approximately 12%. Similar increases
290 in the impact of emissions from the EC and NCP were also found in the four sub-regions.

291 In the Ep2, the GBA was mainly controlled by the sub-tropical high-pressure system, ~~with prevailing southerly~~
292 ~~wind and southerly wind still prevailed~~. However, the ~~low~~ wind speed was ~~low and~~ conducive to the accumulation
293 of the pollutants. Hence, the local sources were the dominant contributors and ~~accounted~~ for about 44%, ~~while~~
294 ~~but~~ the contribution from GDo and neighboring provinces decreased. For O₃ in the GF region, as discussed above,
295 the O₃ in the GF regions is more susceptible to emissions within the GBA under the prevailing southerly wind.
296 Thus, not only the local contribution but also the GBA regional contribution largely increased in the GF region.
297 The regional contribution is larger in the GF region, increasing from 15% to 33%. ~~For the other sub-regions, the~~
298 ~~main increase was in local contributions~~ On the other hand, the main increase in other sub-regions was seen in the
299 ~~local contributions~~.

300

Formatted: Font: Not Italic

301 Table 1. Contribution of pollutants from different source areas to the average hourly O₃ concentration over the
 302 GBA in different cases.

Case	GBA	GDo	Neighbor	Other 1	EC	SWC	NCP	Other 2	Background
Monthly	23%	15%	17%	20%	3%	1%	1%	1%	20%
Ep1	18%	21%	35%	10%	3%	0%	0%	0%	13%
Ep2	44%	11%	7%	27%	0%	0%	0%	0%	11%
Ep3	19%	34%	25%	9%	3%	0%	1%	1%	9%
Ep4	20%	16%	18%	15%	8%	1%	4%	3%	14%

303 * Here, *GDo* represents areas outside the GBA but within Guangdong province. *Neighbor* represents the provinces around
 304 Guangdong province. *Other 1* represents ocean and other countries. *Other 2* represents other areas within the mainland China
 305 in the simulation domain. *Background* represents the contribution of initial and boundary conditions.

306 3.2 Emission Period Contributions

307 The contribution of pollutants emitted from different time periods to the average hourly O₃ concentration in the
 308 GBA and its sub-regions is shown in Figure 4 and Table S3. The background contribution was not considered
 309 in the temporal source contribution analysis. This is because the background contribution is primarily derived
 310 from boundary conditions, and its temporal contribution was calculated based on the time when the pollutants
 311 were transported into D1, rather than the actual emission time.

312 Overall, under the general monthly condition, the emissions within 3 days (namely from Day-0 to Day-2) account
 313 for approximately 73% of the monthly average O₃ concentration within the GBA. The largest proportion of O₃,
 314 around 31%, was formed from the current day's emission (Day-0) and the contribution of pollutants from earlier
 315 emission periods decreases as time elapses. For the monthly average O₃ in different sub-regions, more
 316 O₃ in the GF and SD regions was formed from the emission from Day-0, which contributed about 37% and 36%,
 317 respectively. The contribution of emissions from Day-1 decreased to about 23% in these two regions. The
 318 contribution of Day-0 and Day-1 emissions was relatively small but stable for the HK city and ZZJ region, which
 319 accounted for around 25% and 27%, respectively. The influence of pollutants emitted earlier than 3 days
 320 ago (i.e., Day-4) was generally lower than 20%.

321 The situations are different during the pollution periods. The contribution of emission from the current days to the
 322 average hourly O₃ over the GBA both decreased in the two typhoon cases with similar moving paths (Ep1 and
 323 Ep3). However, the contribution of emissions from Day-1 to Day-3 increased 14% and 8%, respectively. And
 324 the influence of pollutants emitted earlier than 3 days ago (Day-4) decreased 11% in Ep1 and remained almost
 325 unchanged in Ep3. These findings indicate that these two ozone pollutions were caused by the
 326 accumulation of pollutants within the current 3 days.

327 For another typhoon case (Ep4), the contribution from Day-0 decreased approximately by 11%, comparing
 328 with compared to the monthly contribution over the GBA. At the same time, the influence of pollutants from
 329 earlier emitting periods increased, especially for those emitted earlier than 3 days ago (Day-4). It means that the
 330 O₃ pollution during this period was a persistent pollution process. The major contributor should involve not
 331 only the local emissions, but also the long-range transport. Similar variation trend of the temporal contributions
 332 of emission to different sub-regions can be concluded. Similar trends in temporal contribution variations were
 333 observed in different sub-regions, which also illustrated that the O₃ pollution is usually a regional problem.

334 For Ep2, the contribution of emissions from Day-0 increased approximately 18%, while the influence of emissions
 335 from Day-1 to Day-3's emissions decreased about 18%. According to the source area contribution result, the
 336 source area of O₃ over GBA in Ep2 is mainly local sources. Therefore, the contribution of the freshly emitted
 337 pollutants was larger. The contribution of Day-4 emissions to the HK city and ZZJ regions in Ep2 was larger. It
 338 is probably because of the prevailing south wind direction, which brought more airflow from the ocean.
 339 Compared with the emission of the GF and SD regions, the HK city and ZZJ region have lower emission amounts.
 340 At the same time, HK city and ZZJ region were located in the upwind region, and the pollutants from GBA would
 341 have a smaller influence on the O₃ in these two regions. Hence, the amount of fresh pollutants was smaller
 342 and contributed similarly to the Day-4 emissions, which is an accumulated amount.

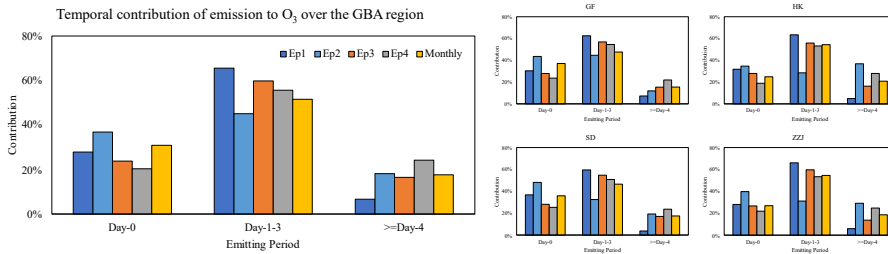


Figure 4. Contribution of pollutants from different emitting periods to the average hourly O₃ concentration over the GBA in different cases.

3.3 Source Area-Time Contributions

To further clarify the relationship between sources and the O₃ concentration in target regions, the evolution of O₃ from various source areas and periods was analyzed. Figure 5 shows the time series of the contributions from different source areas and precursors emission periods to the hourly average O₃ concentration in the GBA region.

Regarding the monthly average O₃ concentration over the GBA, the emissions within the GBA is was the major contributor and generally had have a larger effect on the current day. Under the control of southerly wind, as shown in Figure 6, the pollutants emitted 1 day ago (Day-1) were gradually transported out of the GBA, and the influence of the GBA's emission earlier than Day-1 diminished is much lower. Simultaneously At the same time, the pollutants of GDo and neighboring provinces emitted 1 day ago began to have an impact on the O₃ in the GBA. However, due to the prevailing southerly wind, the impact of aged elder pollutants from GDo and neighboring provinces cannot greatly influence on the O₃ in the GBA was relatively low due to the prevailing southerly wind.

However, regarding the O₃ pollution between 7th and 10th July (Ep1), the major contributors changed. On 7th July, the GBA was under the control of the subtropical high-high-pressure system, and the typhoon was located near the east of Taiwan province. The weather condition was unfavourable for pollutants dispersion, and the O₃ sourced from Day-1 emission within Guangdong provinces was trapped. The prevailing wind shifted to northerly wind, and it also bringing brought some-elder pollutants from neighboring provinces to the GBA. With the approach of the typhoon on from 8th–10th July, the although stronger northwest wind speeded up the diffusion of pollutants from the GBA and deceased the local contribution. However, it also transported more elder pollutants from the northern inland to the GBA. It can be found that the emissions from GDo on the present day also had a significant contribution. At the same time, the pollutants from the neighboring provinces dominated the emissions from Day-1 to Day-3 emissions. Moreover, the pollutants emitted emitting 2 days ago in the eastern-China (EC) region were also transported southwardsoutherly and affected on the O₃ in the of GBA on the current day. Figure 7 shows the spatial distribution of the average source contribution during the Ep1 period. Compared with the monthly average (Figure 6), it was found that the elder pollutants originating from the GBA can be transported back and influence the O₃ concentration in the western part of the GBA during the Ep1 period. This is because easterly and east-winds blew over the GBA from 5th–6th July (Before Ep1, Figure S4). The pollutants emitted within the GBA were transported to northwest inland. However, under the influence of northwest wind, they were transported back to the GBA again. It can also be seen that the pollutants from the GDo 1 day ago were transported downwind quickly, contributing to a high O₃ concentration over the Pearl River Estuary. According to the wind pattern, they mainly came from the northern and western parts of the Guangdong province. Meanwhile, the neighboring provinces' emissions from Day-1 to Day-3 were also transported to the GBA with by the northwest wind, continuously affecting the O₃ over this region.

For the Ep3 O₃ pollution process, results show that the pollutants from GDo and neighboring provinces were also the major contributors. From 30th–31st July, the GBA was under the control of high pressure, and it blew weak north wind prevailed in this region. Afterward, the approaching of the typhoon (1st August) further strengthened the cross-regional transport of pollutants. The difference between Ep3 and Ep1 is that the emissions from GDo have a larger impact on proportion in the Day-1 and Day-2 emissions. Additionally, while pollutants from

385 neighboring provinces and EC in Day-4 emission only accounted for about 5ppb in Ep1, they can still contribute
386 to about 10ppb in Ep3. The possible reason is that northerly wind prevailed over Fujian, Jiangxi, and Hunan
387 provinces during the whole Ep1 period (Figure S4). ~~while~~ However, easterly wind still blew over these provinces
388 during the earlier period of the Ep3 (30th – 31st July, Figure S6), which slowed the transport and influence of
389 pollutants from the neighboring provinces. Generally, the pathways of typhoons in the Ep1 and Ep3 episodes were
390 quite similar, and the influence regions of typhoon wind field mainly covered Guangdong and neighboring
391 provinces. Therefore, the major source area and source time ~~were~~ quite similar in these two cases. To prevent
392 this type of O₃ pollution, earlier emission control (at least 3 days ago) and collaboration with neighboring
393 provinces will gain a better control result.

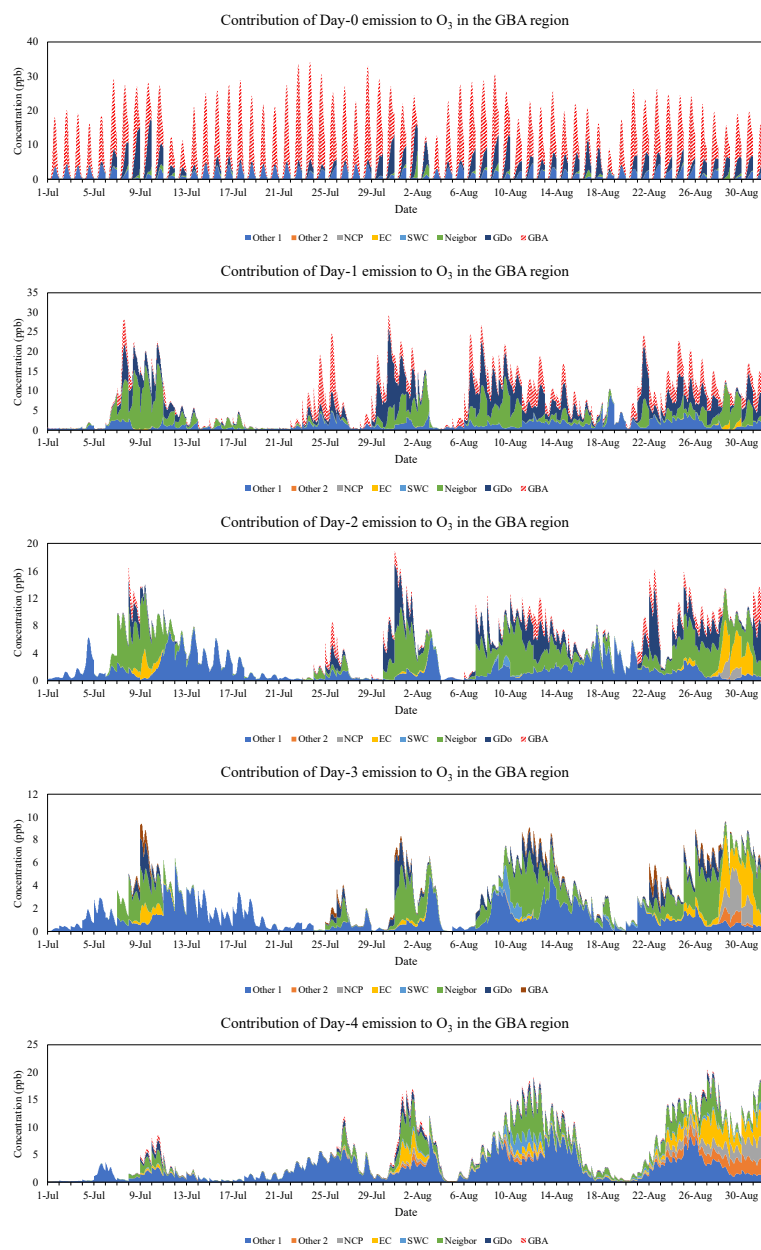
394 On the other hand, the situation is different for the Ep2 ozone pollution. Under the control of ~~the~~ high-pressure
395 system and weak southerly wind (Figure S5), the major contributors were mainly the pollutants from the GBA
396 and the ocean. Unlike the Ep1 and Ep3, the pollutant emitted within the GBA ~~was~~ still dominant in the ~~contribution~~
397 ~~of Day-1's emission-contribution~~. Under the influence of southerly wind, there ~~was minimal migration of is a~~
398 ~~large amount of~~ pollutants ~~migration~~ from north inland ~~regions~~ to the GBA, and the local pollutants were ~~gradually~~
399 ~~dispersing from slowly moving out~~ the GBA. Thus, the pollutant emitted earlier than 2 days ago (\geq Day-2) ~~have~~
400 ~~had~~ a smaller contribution. As shown in Figure 8, the overall diffusion of pollutants within the Guangdong
401 province ~~is was~~ much slower during Ep2. The contribution of ~~the~~ GBA emissions can still reach more than 10 ppb
402 in the Day-1 emission. These results indicate ~~d~~ that this pollution process was mainly driven by the local pollutants
403 within the current 2 days. Hence, emission control should focus on the local sources, and 1-2 days in advance is
404 more efficient.

405 For the last O₃ pollution process (Ep4), ~~which occurred~~ from the 21st to 25th August, ~~the~~ eastern and southern
406 China were mainly controlled by the sub-tropical high-pressure system. ~~At the same time~~ Meanwhile, under the
407 joint influence of peripheral subsidence airflow of typhoon, the wind speed over this region was slow (Figure S7).
408 The weak wind not only trapped the O₃ formed ~~from~~ local emission but also the O₃ formed from cross-regional
409 transported pollutants. The pollutants from ~~the~~ GBA sources mainly dominated the Day-0 and Day-1 emission's
410 contribution, while Day-2 and Day-3 emissions mainly consisted of pollutants from GDo and neighboring
411 provinces. ~~Subsequently, After that, as~~ the typhoon moved ~~northward, northerly and~~ the stronger north~~erly~~
412 wind further broadened the source areas of the O₃ in the GBA (Figure S7). The major contributor of Day-2 and earlier
413 periods' ~~emissions~~ changed to pollutants from the EC and NCP regions. The pollutants emitted earlier than 2
414 days ago from ~~the~~ EC ~~had~~ an important contribution, which accounted for about 12%. Furthermore, the
415 pollutants emitted 3 days ago from the ~~North China Plain (NCP)~~ can also have ~~a noticeable obvious~~ impact on
416 O₃ over the GBA from July 28th– 30th, which can be up to 10%. ~~Hence, to prevent the occurrence of this pollution,~~
417 ~~the emission control region should be further broadened and continuously implemented as it lasted for a longer~~
418 ~~period compared with the other three pollutions. Therefore, to prevent the occurrence of this pollution, emission~~
419 ~~control measures should be implemented in a broader region and continuously enforced, as this pollution episode~~
420 ~~lasted longer compared to the other three cases.~~

421 Figure S8 shows the time series of the contributions from different source areas and precursors' emission periods
422 ~~to for~~ the hourly average O₃ concentration in the GF region and HK city. GF region is located at the inland of the
423 GBA. It is the emission hotspot of the GBA with a higher O₃ concentration (Chen et al., 2022a). HK city ~~is~~ located
424 at the mouth of the PRD. According to previous source apportionment studies (Li et al., 2012, 2013), the pollution
425 in HK city is more attributed to the emissions outside the GBA compared to the other cities of the GBA. Regarding
426 the O₃ in ~~the~~ GF region, ~~the~~ Day-0 emission was usually contributed by ~~both~~ the local emission and ~~the~~ regional
427 transport within the GBA, ~~with which have a~~ similar contributions. The major source areas of the Day-2 to Day-4
428 emissions contributing to ~~the~~ O₃ in ~~the~~ GF in different episodic cases varied similarly to ~~those the ones~~ contributing
429 to the hourly average O₃ in the GBA. Generally, the influence of local and GBA regional pollutants ~~onto~~ O₃ in the
430 GF region ~~diminished rapidly decreased quickly~~ within 1 day. However, the regional emission can still have ~~an~~
431 important contribution in the episodic case ~~that with~~ southerly wind ~~s~~ blew, such as the 24th–25th July (about 26%)
432 in the Ep2 and 23rd–25th (about 15%) in the Ep4. For the O₃ in HK city, the local emission amount is low, and its
433 impact ~~is was~~ also limited to the current day. In addition, the O₃ in HK city ~~is was~~ also susceptible to the impact
434 of pollutants from the ocean but less from the GBA regional emissions. During the Ep1 periods, it was observed
435 that the contribution of the GBA regional sources largely increased in the Day-0 emission as the prevailing wind
436 direction shifted to ~~the~~ north. On the other hand, neighboring provinces' emissions dominated ~~d~~ the contributions
437 of emissions from Day-1 to Day-3. Unlike the GF region, the influence of EC emissions on the O₃ in HK ~~is was~~ also
438 limited in Ep1. Similar conclusions can be drawn for the evolution of the spatiotemporal contribution of emissions

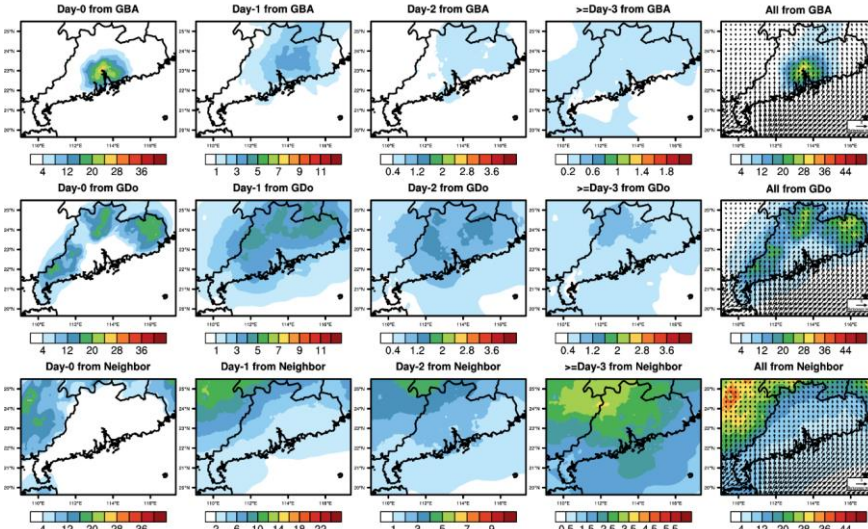
Formatted: English (Hong Kong SAR)

439 in Ep3. As discussed above, the O₃ pollution in Ep2 ~~wasis~~ mainly driven by local emissions. Thus, the O₃
440 concentration in HK city, ~~whieh-is-located~~ in the upwind region with ~~fewersmall~~ local emissions, ~~wasis~~ much
441 lower than the O₃ concentration in the GF region. In Ep4, same as the GBA average and GF region, the impact of
442 pollutants from EC and NCP became important in the Day-2 and Day-3 emissions, which can contribute up to 20%
443 of O₃. These results indicate that although O₃ is usually ~~considered~~ a regional pollution problem, it's necessary to
444 consider the local characteristics of different sub-regions ~~whenwhile~~ making more specific prevention and control
445 policies.



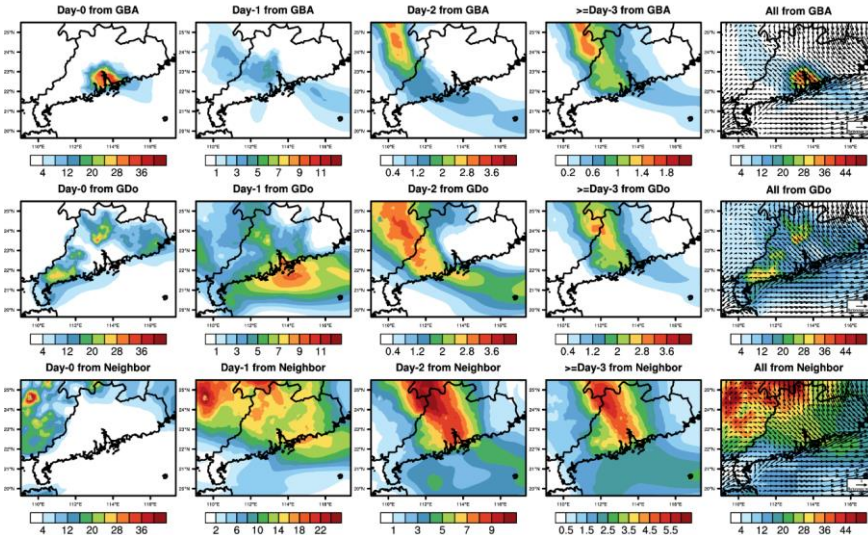
446
 447 Figure 5. Time series of contributions from different source areas and emitting periods to the O₃ concentrations in
 448 the GBA. (*GDo* represents areas outside the GBA region but within Guangdong province. *Neighbor* represents
 449 the provinces around Guangdong province. *Other 1* represents ocean and other countries. *Other 2* represents other
 450 area within the mainland China in the simulation domain.)

Monthly Average O₃ concentration (ppb)



451
 452 Figure 6. Spatial distribution of monthly average O₃ concentration between 9:00-17:00 (Local time) contributed
 453 by emission of GBA, other regions within Guangdong province (GDo), and neighboring provinces (Neighbor)
 454 from various periods. (Unit: ppb. Due to the large variation of contribution, the colorbar range of each sub-figure
 455 is different)

Average O₃ concentration during 7-10 July (ppb)



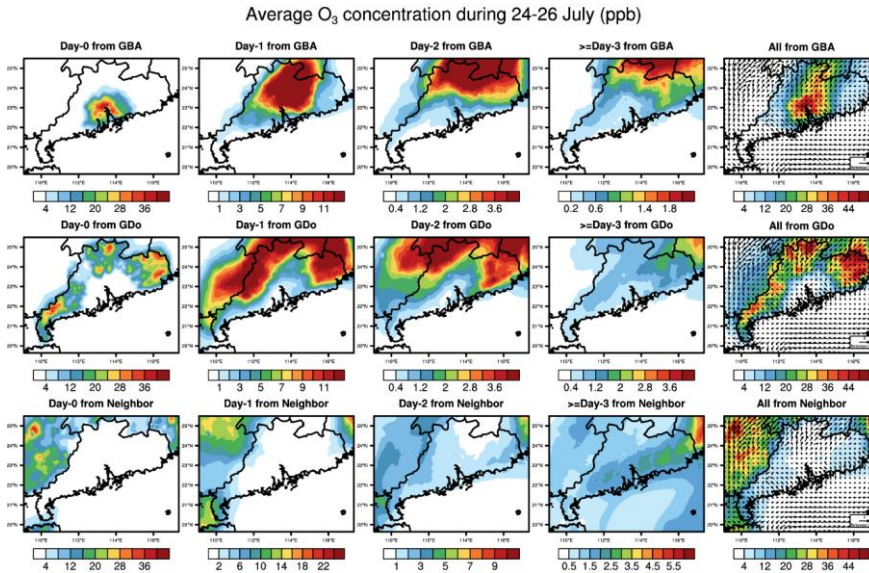
456
 457 Figure 7. Spatial distribution of average O₃ concentration between 9:00-17:00 (Local time) on 7th-10th July 2016
 458 contributed by emission of GBA, other regions within Guangdong province (GDo), and neighboring provinces
 459 (Neighbor) from various periods. (Unit:ppb. The colorbar range of each sub-figure is same as the one in Figure 6)

460
461

Figure 7. Same as Figure 6, but for the period of 7th-10th July 2016

Formatted: Font: Not Italic

Formatted: Centered



462

Figure 8. Spatial distribution of average O₃ concentration between 9:00-17:00 (Local time) on 24th-26th July 2016 contributed by emission of GBA, other regions within Guangdong province (GDo), and neighboring provinces (Neighbor) from various periods. (Unit: ppb. The colorbar range of each sub-figure is same as the one in Figure 6)

463
464
465
466

Figure 8. Same as Figure 6, but for the period of 24th-26th July 2016.

Formatted: Font: Not Italic

Formatted: Centered

467
468

3.4 Verification of the TSA by comparing to Zero-out Experiments

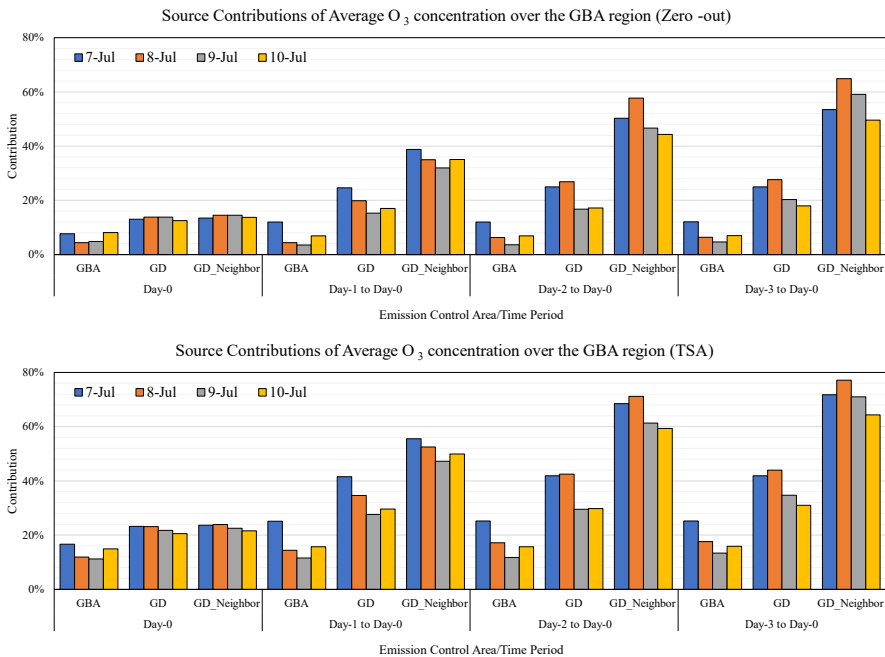
470 Here, the emission zero-out sensitivity experiments, another commonly used method for source apportionment
471 method, were also conducted to evaluate the results from the TSA method. The zero-out method needs to conduct
472 two sets of simulations, including the control run and the zero-out run. In the control run, the simulations were
473 conducted using the complete emissions. In the zero-out runs, the simulations were conducted with the emissions
474 that specific period and area were removed. Subsequently After that, the contribution of the specific source area
475 and source time was derived by calculating the difference between the control and zero-out simulations. For each
476 target date, the emission control area was set as the GBA, Guangdong province (GD), Guangdong and neighboring
477 provinces (GD_Neighbor), respectively. For each target date, three types of emission area controls were
478 implemented: Type 1 involved the GBA region alone (GBA); Type 2 included the emission within Guangdong
479 province (GD, namely GBA+GDo); and Type 3 expanded to encompass the emission within Guangdong province
480 and neighbouring provinces (GD_Neighbor, namely GBA + GDo + Neighbor). The emission control period was
481 set as continuous control beginning from the current day, which is also the target day (Day-0), from 1 day ago
482 (Day-1), from 2 days ago (Day-2) and from 3 days ago (Day-3), respectively. The zero-out experiments were
483 carried out for the periods between 7th and 10th July (Typhoon case) and between 24th and 26th (Sub-tropical high
484 case). More configurations can be found in Tables S4- S5.

485 From the result of zero-out experiments (Fig.9 and Fig.S9), it can be seen that, for the typhoon case (Fig.9), when
486 only controlling the emission within the GBA, there is little difference between results of controlling emissions 1
487 day in advance and 3 days in advance. This is consistent with the TSA result that the influence of the emission
488 within the GBA is usually limited to 2 days. The effect of controlling emission 1 day ahead in GD is better than

489 that of only GBA Controlling emissions 1 day in advance in GD yields better results compared to solely controlling
 490 emissions within the GBA. There is less variation of the O₃ concentration when controlling the emission within
 491 GD Guangdong province 2 days or 3 days in advance. Meanwhile, regarding only controlling emissions control
 492 on from the Day-0, there is it shows limited improvement in controlling the emission for a larger area (GD and
 493 GD Neighbor) than solely within the GBA. This result aligns with It's the same as the TSA result that the
 494 pollutants from neighboring provinces took effect on the O₃ over the GBA region at least 1 day later. Joint control
 495 from Guangdong and neighboring province (GD Neighbor) has a larger better optimal effect in the simulations
 496 conducted from Day-2 to Day-0 and Day-3 to Day-0 simulations. And the difference between GD Neighbor
 497 and the GD result is also more pronounced obvious in these simulations, indicating that it's more effective to
 498 implement joint control within other provinces 2-3 days in advance.

499 For the sub-tropical high case (Fig.S9), whatever controlling the emissions on the current day or 2 days ahead,
 500 the effect of solely only controlling emissions within the GBA is similar to those that of joint control in a larger
 501 area (GD and GD Neighbor). It supports our previous conclusion that the pollution is mainly contributed by the
 502 local sources. Additionally, At the same time, there is limited optimization effect to control the emission 2-3 days
 503 in advance than controlling 1 days in advance. To alleviate this ozone pollution, controlling the local emission
 504 within the short term should be effective. Although the contribution discrepancies between the source
 505 contribution (%) calculated from the zero-out method and those obtained one from the TSA method can reach
 506 20%, which is due to the non-linear chemistry relationship between ozone and its precursors, as well as and the
 507 differences in the methodology mechanism of different methods (Kwok et al., 2015; Clappier et al., 2017), similar
 508 relationships between source area/time and receptor can be drawn. These results also support the validity of the
 509 TSA approach.

510



511
 512 Figure 9. The contribution of different source areas and time periods to the O₃ concentration over the GBA in the
 513 typhoon case using the zero-out and TSA methods. (Different colors represent different target dates; Upper: Zero-
 514 out; Bottom: TSA)

515

516 **3.5 Discussion**

517 Previous studies mainly focused on exploring the contribution and control of various source areas and categories
518 on O₃ over the GBA. The analysis in this study illustrated that there could be a larger difference between the
519 temporal contribution of emissions to the O₃ pollution over the GBA under different weather patterns. ~~It indicates~~
520 ~~that understanding the contribution of pollutants from different emitting periods and finding out the major period~~
521 ~~is also crucial in control policymaking, especially in episodic cases. This finding emphasizes the importance of~~
522 ~~understanding the contribution of pollutants from different emission periods and identifying the major periods,~~
523 ~~particularly in episodic cases, for effective policymaking in pollution control. Different from the zero-out method~~
524 ~~that needs sets of simulations, it can provide an overall picture of source contributions within one simulation,~~
525 ~~saving more computation costs, and is suitable for applications in which more potential sources are considered.~~
526 ~~In contrast to the zero-out method, which requires multiple simulations, our approach provides a comprehensive~~
527 ~~overview of source contributions within a single simulation. This method is suited for applications involving more~~
528 ~~potential sources as it saves computation costs.~~

529 In addition, meteorological conditions play an important role in affecting the effectiveness of the emission control
530 area and period. The results here suggest that the approach of typhoons usually strengthens the cross-region
531 transportation of pollutants to the GBA. Therefore, cross-province collaboration and control should be
532 implemented at least 2-3 days ahead when the typhoon is predicted. ~~The information obtained from the TSA results~~
533 ~~can contribute to the establishment of an early warning and rapid response system. It could help to facilitate~~
534 ~~collaboration, considering estimated timelines and the cost implications associated with emission reduction efforts,~~
535 ~~aiming to achieve a balanced outcome across regions. In contrast, local emission control within 2 days is more~~
536 ~~effective when the GBA is under the influence of a high-pressure system. The primary focus for emission control~~
537 ~~measures should be on local vehicles and industries, as they are the major contributors of NO_x and VOCs (Bian~~
538 ~~et al., 2019; Li et al., 2019). Implementing measures such as traffic restrictions based on even- and odd-numbered~~
539 ~~license plates and temporary reduction of emissions from industries can be effective strategies to target these~~
540 ~~sources in advance. Our findings emphasize the importance of considering the impact of meteorological~~
541 ~~conditions when implementing control measures in advance. Here, our study primarily focuses on the summer~~
542 ~~season, which has been identified as the O₃ pollution period in the GBA (Gao et al., 2018; Li et al., 2022).~~
543 ~~Typhoons and subtropical high-pressure systems are two significant weather patterns closely linked with O₃~~
544 ~~pollution events in Southern China (Wang et al., 2017; Ouyang et al., 2022). The trajectories of typhoons in~~
545 ~~episodes 1 and 3 (Figure S3) are similar to one of the typical typhoon pathways, often coinciding with O₃ pollution~~
546 ~~events in the GBA (Qu et al., 2021; Wang et al., 2022a). Meanwhile, the high 2-m temperature and low 2-m~~
547 ~~relative humidity over the GBA can be observed during the O₃ episodes (Figure S10-S11). The prevailing wind~~
548 ~~across the GBA in the typhoon and sub-tropical high-pressure cases is northerly and southerly, respectively~~
549 ~~(Figures S12). Overall, the weather conditions observed in the selected cases of this study are similar to those~~
550 ~~reported in other O₃ pollution studies in this region (Qu et al., 2021; Ouyang et al., 2022; Wang et al., 2022).~~
551 ~~Nevertheless, it is crucial to underscore that the spatial-temporal source contribution may vary in O₃ pollutions~~
552 ~~even under similar meteorological conditions. For instance, the change of typhoon position and intensity could~~
553 ~~influence the large-scale circulation and precursor emission (Zhan et al., 2020; Wang et al., 2022a). Therefore, it~~
554 ~~is imperative to undertake further investigations and comparative studies on more similar O₃ events over the GBA~~
555 ~~under the influence of typhoons and subtropical high-pressures in the future, which will contribute to attaining~~
556 ~~more widely applicable findings and offer valuable insights for developing emission control strategies. The TSA~~
557 ~~method could help to better understand the spatial-temporal sources of O₃ pollution under the current emission~~
558 ~~level. It will provide scientific references for designing of effective and timely control policies when unfavorable~~
559 ~~weather conditions are predicted. So, Additionally, the spatial-temporal influence of emission to O₃ over the GBA~~
560 ~~under other unfavourable conditions and seasons is also essential to further explore through the TSA method,~~
561 ~~which helps to gain a more comprehensive understanding of when and where the O₃ over the GBA comes from.~~

562 ~~In the context Under the background~~ of climate change, ~~the occurrence of~~ extreme weather, such as extreme
563 heatwaves (Coffel et al., 2018; Dong et al., 2023), ~~may occur~~ ~~is expected to become~~ more frequently. ~~These~~
564 ~~events which~~ will ~~significantly~~ ~~largely~~ impact the sources and sinks of pollutants ~~by different~~ ~~through various~~
565 physical and chemical processes. At the same time, ~~governments in different countries will implement~~ various
566 emission control strategies ~~in response to responding to~~ climate change, such as carbon neutrality (Liu et al., 2021;
567 Zhang et al., 2021), ~~will be implemented by governments in different countries,~~ which will also ~~change~~ ~~alter~~ the
568 ~~emission structure of emissions.~~ How these extreme weather events and control measures influence the temporal
569 characterization of sources, ~~and the~~ formation of air pollution, ~~and as well as~~ the spatial-temporal contribution of

Formatted: Font: Not Italic

Formatted: Font: Not Italic

Formatted: Font: Not Italic, Subscript

Formatted: Font: Not Italic

Formatted: Font: Not Italic

Formatted: Font: Not Italic

Formatted: Font: Not Italic

Formatted: Font: Not Italic

Formatted: Font: Not Italic

Formatted: Font: Not Italic

570 emissions from different countries ~~and, as well as~~ their interactions, are also worth further investigation in the
571 future. ~~Such investigations~~It can ~~foster~~~~promote~~ the mutual cooperation among nations to ~~collectively address~~
572 ~~environmental challenges, combat the environmental issues together.~~

573 However, it should be noted that the numerical model source apportionment results are usually influenced by the
574 uncertainties of the emission inventory as most of the emission inventories are ~~constructed~~~~built-up~~ by the bottom-
575 up method and cannot be updated in a timely manner. With the increasing availability of different types of
576 observations, including surface monitoring and satellite remote sensing data, different top-down methods such as
577 data assimilation (East et al., 2022) and machine learning (Chen et al., 2023) have been applied to integrate
578 observations and optimize the emissions. These methods should be implemented to update the emission inventory
579 ~~and combined with the TSA method to evaluate the evolution of spatial-temporal sources in different historical~~
580 ~~periods and provide up-to-date source information for policymaking.~~ ~~Meanwhile, the air quality model results are~~
581 ~~also sensitive to the uncertainty in the weather forecast, potentially leading to variations in source apportionment~~
582 ~~results. To alleviate the impact of weather forecast uncertainty, different methods, such as ensemble simulation~~
583 ~~(Gilliam et al., 2015), data assimilation for the meteorological field simulation (Kwon et al., 2018), and machine~~
584 ~~learning method (Scher et al., 2018; Cho et al., 2020), should be applied to enhance the accuracy of meteorological~~
585 ~~field simulations.~~

586
587

588 4. Conclusion

589 In this study, we applied the CAMx-TSA method to analyze the spatial and temporal contribution of different
590 sources to the O₃ pollution in the GBA ~~during~~in summer. The result shows that the O₃ over the GBA in summer is
591 mainly contributed by the pollutants from local emissions, followed by ~~pollutants originating from~~ other regions
592 within Guangdong province (~~GDo~~) and neighbouring provinces. ~~The O₃ was usually formed by the pollutants~~
593 ~~emitted within 3 days, which account for more than 70%. The O₃ formation is predominantly attributed to~~
594 ~~pollutants emitted within a 3-day period, accounting for over 70% of the total contribution.~~ During the O₃ episodes,
595 when the typhoon moved from the eastern Philippine Sea ~~towards~~to southern China, the prevailing wind shifted
596 from south to north over the GBA. ~~It conducive more~~This facilitated the transport of pollutants ~~transported~~ from
597 GDo and neighbouring provinces to the GBA, ~~resulting in leading to~~an increase in O₃ concentrations. The
598 pollutants emitted 3 days ago still have a significant contribution. ~~When~~While the typhoon ~~remained just stayed~~
599 near the sea areas east of Taiwan province and moved ~~northward~~~~northly~~, under the continuous influence of
600 northerly wind, the emissions ~~from~~of eastern China, even the North China Plain from 3 days ago can also have an
601 ~~noticeable~~~~obvious~~ impact on O₃ over the GBA. In contrast, when the GBA ~~was~~is mainly under the control of ~~the~~
602 sub-tropical high-pressure system, the ozone pollution was mainly caused by the local pollutants within the current
603 2 days. The results indicated that ~~implementing~~ joint emission control ~~action~~measures with other provinces 2-3
604 days in advance is more effective for preventing the O₃ pollution in the GBA when the typhoon is ~~approaching~~
605 ~~moving towards~~ southern China. On the other hand, it's more efficient to pay more attention to local sources
606 control within 2 days when the GBA is under the control of the high-pressure system.

607 Here, different surrounding provinces were categorized as one source area here to save computation resource for
608 more potential source investigation. As the neighbouring province was illustrated as a major contributor to the O₃
609 in the GBA, it is necessary to further divided this source into several sub-source areas and explore their individual
610 impact in future work. ~~Meanwhile, our preliminary findings indicate that pollutants emitted more than three days~~
611 ~~prior can still have a considerable impact on the O₃ levels in the GBA. As a result, it would be valuable to conduct~~
612 ~~source apportionment analyses with finer source areas and earlier source periods for O₃ pollution in different cities~~
613 ~~within the GBA. This further investigation would provide deeper insights into the unique O₃ pollution~~
614 ~~characteristics of each city.~~ In addition, individual source categories were not separated in this study, mainly due
615 to the application of different emission inventories with different source category classifications, making it
616 difficult to combine them. It is important to note that each source category has its own characteristic temporal
617 profile, which can have different temporal impacts on O₃ concentrations. Therefore, the temporal contribution of
618 various source categories, including anthropogenic and biogenic emissions, should be also considered in future
619 work. These works can provide more spatial and temporal information of O₃ source over the GBA, ~~enabling local~~
620 ~~governments to design and implement more targeted control measures more effectively and promptly~~to the local
621 ~~governments so that the targeted control measures can be designed and implemented more effectively and timely.~~

Formatted: Font: Not Italic

Formatted: Font: Not Italic

Formatted: Font: Not Italic

Formatted: Font: Not Italic

622

623 Code and Data availability

624 Hourly O₃ observation data were released by the China National Environmental Monitoring Centre
625 (<http://www.cnemc.cn/en>, last access 24 December; CNEMC, 2023) and the Hong Kong Environmental
626 Protection Department (<https://cd.epic.epd.gov.hk/EPICDI/air/station/?lang=en>, last access 24 December 2023;
627 HKEPD, 2023). The CAMx model code is freely available via <https://www.camx.com/download/>, last access 24
628 December, 2023). The ECMWF Reanalysis v5 (ERA5) data was downloaded from
629 <https://www.ecmwf.int/en/forecasts/dataset/ecmwf-reanalysis-v5>, last access 17 May 2024; ERA5, 2024)

630

631 Author contribution

632 CY, LX, and JF designed the research. CY contributed to model development, simulation and data analysis. LX
633 and JF contributed to the result discussion. CY prepared the manuscript with contributions from all co-authors.

634

635 Competing interests

636 The authors declare that they have no conflict of interest.

637

638 Acknowledgements

639 This work was supported by the Research Grants Council of Hong Kong Government (C6026-22GF) and the
640 Improvement on Competitiveness in Hiring New Faculties Funding Scheme of CUHK (No. 4937115)

641

642 References

- 643 [Bian, Y., Huang, Z., Ou, J., Zhong, Z., Xu, Y., Zhang, Z., Xiao, X., Ye, X., Wu, Y., Yin, X., Li, C., Chen, L., Shao,
644 M., and Zheng, J.: Evolution of anthropogenic air pollutant emissions in Guangdong Province, China, from 2006
645 to 2015, *Atmospheric Chemistry and Physics*, 19, 11701-11719, 10.5194/acp-19-11701-2019, 2019.](#)
- 646 Cao, M., Fan, S., Jin, C., Cai, Q., and He, Y.: O₃ pollution characteristics, weather classifications and local
647 meteorological conditions in Guangdong from 2015 to 2020, *Acta Scientiae Circumstantiae*, 43, 19-31,
648 10.13671/j.hjkxxb.2022.0416, 2023. (in Chinese)
- 649 Cao, T., Wang, H., Li, L., Lu, X., Liu, Y., and Fan, S.: Fast spreading of surface ozone in both temporal and spatial
650 scale in Pearl River Delta, *Journal of Environmental Sciences*, 137, 540-552, 10.1016/j.jes.2023.02.025, 2024.
- 651 Chen, W., Chen, Y., Chu, Y., Zhang, J., Xian, C., Lin, C., Fung, Z., and Lu, X.: Numerical simulation of ozone
652 source characteristics in the Pearl River Delta region, *Acta Scientiae Circumstantiae*, 42, 293-308,
653 10.13671/j.hjkxxb.2021.0328, 2022a. (in Chinese)
- 654 Chen, X., Wang, N., Wang, G., Wang, Z., Chen, H., Cheng, C., Li, M., Zheng, L., Wu, L., Zhang, Q., Tang, M.,
655 Huang, B., Wang, X., and Zhou, Z.: The Influence of Synoptic Weather Patterns on Spatiotemporal Characteristics
656 of Ozone Pollution Across Pearl River Delta of Southern China, *Journal of Geophysical Research: Atmospheres*,
657 127, 10.1029/2022jd037121, 2022b.
- 658 Chen, Y., Fung, J. C. H., Huang, Y., Lu, X., Wang, Z., Louie, P. K. K., Chen, W., Yu, C. W., Yu, R., and Lau, A. K.
659 H.: Temporal Source Apportionment of PM_{2.5} Over the Pearl River Delta Region in Southern China, *Journal of*
660 *Geophysical Research: Atmospheres*, 127, 10.1029/2021jd035271, 2022c.
- 661 Chen, Y., Fung, J. C. H., Yuan, D., Chen, W., Fung, T., and Lu, X.: Development of an integrated machine-learning
662 and data assimilation framework for NO_x emission inversion, *Science of The Total Environment*, 871,
663 10.1016/j.scitotenv.2023.161951, 2023.

Formatted: English (United States)

Formatted: English (Hong Kong SAR)

664 [Cho, D., Yoo, C., Im, J., and Cha, D. H.: Comparative Assessment of Various Machine Learning-Based Bias](#)
665 [Correction Methods for Numerical Weather Prediction Model Forecasts of Extreme Air Temperatures in Urban](#)
666 [Areas, Earth and Space Science, 7, 10.1029/2019ea000740, 2020.](#)

667 Clappier, A., Belis, C. A., Pernigotti, D., and Thunis, P.: Source apportionment and sensitivity analysis: two
668 methodologies with two different purposes, *Geoscientific Model Development*, 10, 4245-4256, 10.5194/gmd-10-
669 4245-2017, 2017.

670 CNEMC: China National Environmental Monitoring Centre: Real-time National Air Quality,
671 <http://www.cnemc.cn/en>, last access: 24 December 2023.

672 Coffel, E. D., Horton, R. M., and de Sherbinin, A.: Temperature and humidity based projections of a rapid rise in
673 global heat stress exposure during the 21st century, *Environmental Research Letters*, 13, 10.1088/1748-
674 9326/aaa00e, 2018.

675 Deng, T., Wang, T., Wang, S., Zou, Y., Yin, C., Li, F., Liu, L., Wang, N., Song, L., Wu, C., and Wu, D.: Impact of
676 typhoon periphery on high ozone and high aerosol pollution in the Pearl River Delta region, *Science of The Total*
677 *Environment*, 668, 617-630, 10.1016/j.scitotenv.2019.02.450, 2019.

678 Dong, W., Jia, X., Qian, Q., and Li, X.: Rapid Acceleration of Dangerous Compound Heatwaves and Their Impacts
679 in a Warmer China, *Geophysical Research Letters*, 50, 10.1029/2023gl104850, 2023.

680 East, J. D., Henderson, B. H., Napelenok, S. L., Koplitz, S. N., Sarwar, G., Gilliam, R., Lenzen, A., Tong, D. Q.,
681 Pierce, R. B., and Garcia-Menendez, F.: Inferring and evaluating satellite-based constraints on NO_x emissions
682 estimates in air quality simulations, *Atmospheric Chemistry and Physics*, 22, 15981-16001, 10.5194/acp-22-
683 15981-2022, 2022.

684 Emery, C., Tai, E., and Yarwood, G.: Enhanced meteorological modeling and performance evaluation for two
685 Texas ozone episodes, Prepared for the Texas natural resource conservation commission, by ENVIRON
686 International Corporation, 2001.

687 EPA, U.: Guidance on the use of models and other analyses for demonstrating attainment of air quality goals for
688 ozone, PM_{2.5}, and regional haze, Technical Support Document, 2007.

689 [ERA5, ECMWF Reanalysis v5 data, https://www.ecmwf.int/en/forecasts/dataset/ecmwf-reanalysis-v5, last access](https://www.ecmwf.int/en/forecasts/dataset/ecmwf-reanalysis-v5)
690 [17 May 2024; ERA5, 2024](#)

691 Fang, T., Zhu, Y., Wang, S., Xing, J., Zhao, B., Fan, S., Li, M., Yang, W., Chen, Y., and Huang, R.: Source impact
692 and contribution analysis of ambient ozone using multi-modeling approaches over the Pearl River Delta region,
693 China, *Environmental Pollution*, 289, 10.1016/j.envpol.2021.117860, 2021.

694 Feng, X., Guo, J., Wang, Z., Gu, D., Ho, K.-F., Chen, Y., Liao, K., Cheung, V. T. F., Louie, P. K. K., Leung, K. K.
695 M., Yu, J. Z., Fung, J. C. H., and Lau, A. K. H.: Investigation of the multi-year trend of surface ozone and ozone-
696 precursor relationship in Hong Kong, *Atmospheric Environment*, 315, 10.1016/j.atmosenv.2023.120139, 2023.

697 Gao, X., Deng, X., Tan, H., Wang, C., Wang, N., and Yue, D.: Characteristics and analysis on regional pollution
698 process and circulation weather types over Guangdong Province, *Acta Scientiae Circumstantiae*, 38, 1708-1716,
699 10.13671/j.hjkxxb.2017.0473, 2018. (in Chinese)

700 [Gilliam, R. C., Hogrefe, C., Godowitch, J. M., Napelenok, S., Mathur, R., and Rao, S. T.: Impact of inherent](#)
701 [meteorology uncertainty on air quality model predictions, Journal of Geophysical Research: Atmospheres, 120,](#)
702 [10.1002/2015jd023674, 2015.](#)

703 Gong, C., Liao, H., Yue, X., Ma, Y., and Lei, Y.: Impacts of Ozone-Vegetation Interactions on Ozone Pollution
704 Episodes in North China and the Yangtze River Delta, *Geophysical Research Letters*, 48, 10.1029/2021gl093814,
705 2021.

706 Gong, S., Zhang, L., Liu, C., Lu, S., Pan, W., and Zhang, Y.: Multi-scale analysis of the impacts of meteorology
707 and emissions on PM_{2.5} and O₃ trends at various regions in China from 2013 to 2020. Key weather elements and
708 emissions, *Science of The Total Environment*, 824, 10.1016/j.scitotenv.2022.153847, 2022.

Formatted: English (Hong Kong SAR)

709 Han, H., Liu, J., Shu, L., Wang, T., and Yuan, H.: Local and synoptic meteorological influences on daily variability
710 in summertime surface ozone in eastern China, *Atmospheric Chemistry and Physics*, 20, 203-222, 10.5194/acp-
711 20-203-2020, 2020.

712 He, Z., Wang, X., Ling, Z., Zhao, J., Guo, H., Shao, M., and Wang, Z.: Contributions of different anthropogenic
713 volatile organic compound sources to ozone formation at a receptor site in the Pearl River Delta region and its
714 policy implications, *Atmospheric Chemistry and Physics*, 19, 8801-8816, 10.5194/acp-19-8801-2019, 2019.

715 HKPD, Hong Kong Air Quality Data, <https://cd.epic.epd.gov.hk/EPICDI/air/station/?lang=en>, last access: 24
716 December 2023)

717 Kwok, R., Baker, K., Napelenok, S., and Tonnesen, G.: Photochemical grid model implementation and application
718 of VOC, NO_x, and O₃ source apportionment, *Geoscientific Model Development*, 8, 99-114, 2015.

719 [Kwon, I.-H., English, S., Bell, W., Potthast, R., Collard, A., and Ruston, B.: Assessment of Progress and Status of
720 Data Assimilation in Numerical Weather Prediction, *Bulletin of the American Meteorological Society*, 99, ES75-
721 ES79, 10.1175/bams-d-17-0266.1, 2018.](#)

722 Li, M., Liu, H., Geng, G., Hong, C., Liu, F., Song, Y., Tong, D., Zheng, B., Cui, H., Man, H., Zhang, Q., and He,
723 K.: Anthropogenic emission inventories in China: a review, *National Science Review*, 4, 834-866,
724 10.1093/nsr/nwx150, 2017.

725 [Li, M., Zhang, Q., Zheng, B., Tong, D., Lei, Y., Liu, F., Hong, C., Kang, S., Yan, L., Zhang, Y., Bo, Y., Su, H.,
726 Cheng, Y., and He, K.: Persistent growth of anthropogenic non-methane volatile organic compound \(NMVOC\)
727 emissions in China during 1990–2017: drivers, speciation and ozone formation potential, *Atmospheric Chemistry
728 and Physics*, 19, 8897-8913, 10.5194/acp-19-8897-2019, 2019.](#)

729 [Li, T., Chen, J., Weng, J., Shen, J., and Gong, Y.: Ozone pollution synoptic patterns and their variation
730 characteristics in Guangdong Province, *China Environmental Science*, 42, 2015-2024, 10.19674/j.cnki.issn1000-
731 6923.2022.0102, 2022. \(in Chinese\)](#)

732 Li, Y., Lau, A. K. H., Fung, J. C. H., Zheng, J. Y., Zhong, L. J., and Louie, P. K. K.: Ozone source apportionment
733 (OSAT) to differentiate local regional and super-regional source contributions in the Pearl River Delta region,
734 China, *Journal of Geophysical Research: Atmospheres*, 117, 10.1029/2011jd017340, 2012.

735 Li, Y., Lau, A. K. H., Fung, J. C. H., Ma, H., and Tse, Y.: Systematic evaluation of ozone control policies using an
736 Ozone Source Apportionment method, *Atmospheric Environment*, 76, 136-146, 10.1016/j.atmosenv.2013.02.033,
737 2013.

738 Li, Y., Zhao, X., Deng, X., and Gao, J.: The impact of peripheral circulation characteristics of typhoon on sustained
739 ozone episodes over the Pearl River Delta region, China, *Atmospheric Chemistry and Physics*, 22, 3861-3873,
740 10.5194/acp-22-3861-2022, 2022.

741 Lin, X., Yuan, Z., Yang, L., Luo, H., and Li, W.: Impact of Extreme Meteorological Events on Ozone in the Pearl
742 River Delta, China, *Aerosol and Air Quality Research*, 19, 1307-1324, 10.4209/aaqr.2019.01.0027, 2019.

743 Liu, H., Zhang, M., and Han, X.: A review of surface ozone source apportionment in China, *Atmospheric and
744 Oceanic Science Letters*, 13, 470-484, 10.1080/16742834.2020.1768025, 2020a.

745 Liu, Y. and Wang, T.: Worsening urban ozone pollution in China from 2013 to 2017 – Part 1: The complex and
746 varying roles of meteorology, *Atmospheric Chemistry and Physics*, 20, 6305-6321, 10.5194/acp-20-6305-2020,
747 2020b.

748 Liu, Y., Geng, G., Cheng, J., Liu, Y., Xiao, Q., Liu, L., Shi, Q., Tong, D., He, K., and Zhang, Q.: Drivers of
749 Increasing Ozone during the Two Phases of Clean Air Actions in China 2013–2020, *Environmental Science &
750 Technology*, 57, 8954-8964, 10.1021/acs.est.3c00054, 2023.

Formatted: English (Hong Kong SAR)

Formatted: English (Hong Kong SAR)

- 752 Liu, Z., Deng, Z., He, G., Wang, H., Zhang, X., Lin, J., Qi, Y., and Liang, X.: Challenges and opportunities for
753 carbon neutrality in China, *Nature Reviews Earth & Environment*, 3, 141-155, 10.1038/s43017-021-00244-x,
754 2021.
- 755 Lu, X., Yao, T., Li, Y., Fung, J. C. H., and Lau, A. K. H.: Source apportionment and health effect of NO_x over the
756 Pearl River Delta region in southern China, *Environmental Pollution*, 212, 135-146,
757 10.1016/j.envpol.2016.01.056, 2016.
- 758 Lu, X., Zhang, L., and Shen, L.: Meteorology and Climate Influences on Tropospheric Ozone: a Review of Natural
759 Sources, Chemistry, and Transport Patterns, *Current Pollution Reports*, 5, 238-260, 10.1007/s40726-019-00118-
760 3, 2019.
- 761 Maji, K. J., Ye, W.-F., Arora, M., and Nagendra, S. M. S.: Ozone pollution in Chinese cities: Assessment of
762 seasonal variation, health effects and economic burden, *Environmental Pollution*, 247, 792-801,
763 10.1016/j.envpol.2019.01.049, 2019.
- 764 Ouyang, S., Deng, T., Liu, R., Chen, J., He, G., Leung, J. C.-H., Wang, N., and Liu, S. C.: Impact of a subtropical
765 high and a typhoon on a severe ozone pollution episode in the Pearl River Delta, China, *Atmospheric Chemistry
766 and Physics*, 22, 10751-10767, 10.5194/acp-22-10751-2022, 2022.
- 767 Qu, K., Wang, X., Yan, Y., Shen, J., Xiao, T., Dong, H., Zeng, L., and Zhang, Y.: A comparative study to reveal
768 the influence of typhoons on the transport, production and accumulation of O₃ in the Pearl River Delta, China,
769 *Atmospheric Chemistry and Physics*, 21, 11593-11612, 10.5194/acp-21-11593-2021, 2021.
- 770 Sahu, S. K., Liu, S., Liu, S., Ding, D., and Xing, J.: Ozone pollution in China: Background and transboundary
771 contributions to ozone concentration & related health effects across the country, *Science of The Total Environment*,
772 761, 10.1016/j.scitotenv.2020.144131, 2021.
- 773 [Scher, S. and Messori, G.: Predicting weather forecast uncertainty with machine learning, *Quarterly Journal of
774 the Royal Meteorological Society*, 144, 2830-2841, 10.1002/qj.3410, 2018.](#)
- 775 Wang, N., Huang, X., Xu, J., Wang, T., Tan, Z.-m., and Ding, A.: Typhoon-boosted biogenic emission aggravates
776 cross-regional ozone pollution in China, *Science Advances*, 8, eabl6166, 2022a.
- 777 Wang, T., Xue, L., Brimblecombe, P., Lam, Y. F., Li, L., and Zhang, L.: Ozone pollution in China: A review of
778 concentrations, meteorological influences, chemical precursors, and effects, *Science of The Total Environment*,
779 575, 1582-1596, 10.1016/j.scitotenv.2016.10.081, 2017.
- 780 Wang, T., Xue, L., Feng, Z., Dai, J., Zhang, Y., and Tan, Y.: Ground-level ozone pollution in China: a synthesis of
781 recent findings on influencing factors and impacts, *Environmental Research Letters*, 17, 10.1088/1748-
782 9326/ac69fe, 2022b.
- 783 Wang, Y., Wild, O., Ashworth, K., Chen, X., Wu, Q., Qi, Y., and Wang, Z.: Reductions in crop yields across China
784 from elevated ozone, *Environmental Pollution*, 292, 10.1016/j.envpol.2021.118218, 2022c.
- 785 [Wang, W., Parrish, D. D., Wang, S., Bao, F., Ni, R., Li, X., Yang, S., Wang, H., Cheng, Y., and Su, H.: Long-term
786 trend of ozone pollution in China during 2014–2020: distinct seasonal and spatial characteristics and ozone
787 sensitivity, *Atmospheric Chemistry & Physics*, 22, 8935-8949, 10.5194/acp-22-8935-2022, 2022d.](#)
- 788 Wu, Y., Chen, W., You, Y., Xie, Q., Jia, S., and Wang, X.: Quantitative impacts of vertical transport on the long-
789 term trend of nocturnal ozone increase over the Pearl River Delta region during 2006–2019, *Atmospheric
790 Chemistry and Physics*, 23, 453-469, 10.5194/acp-23-453-2023, 2023.
- 791 Xie, X., Shi, Z., Ying, Q., Zhang, H., and Hu, J.: Age-Resolved Source and Region Contributions to Fine
792 Particulate Matter During an Extreme Haze Episode in China, *Geophysical Research Letters*, 48,
793 10.1029/2021gl095388, 2021.
- 794 Xie, X., Hu, J., Qin, M., Guo, S., Hu, M., Ji, D., Wang, H., Lou, S., Huang, C., Liu, C., Zhang, H., Ying, Q., Liao,
795 H., and Zhang, Y.: Evolution of atmospheric age of particles and its implications for the formation of a severe
796 haze event in eastern China, *Atmospheric Chemistry and Physics*, 23, 10563-10578, 10.5194/acp-23-10563-2023,
797 2023.

Formatted: English (Hong Kong SAR)

798 Xu, J., Zhao, Z., Wu, Y., Zhang, Y., Wang, Y., Su, B., Liang, Y., Hu, T., and Liu, R.: Impacts of Meteorological
799 Conditions on Autumn Surface Ozone During 2014–2020 in the Pearl River Delta, China, *Earth and Space Science*,
800 10, 10.1029/2022ea002742, 2023a.

801 Xu, Y., Shen, A., Jin, Y., Liu, Y., Lu, X., Fan, S., Hong, Y., and Fan, Q.: A quantitative assessment and process
802 analysis of the contribution from meteorological conditions in an O₃ pollution episode in Guangzhou, China,
803 *Atmospheric Environment*, 303, 10.1016/j.atmosenv.2023.119757, 2023b.

804 Yang, J. and Zhao, Y.: Performance and application of air quality models on ozone simulation in China – A review,
805 *Atmospheric Environment*, 293, 10.1016/j.atmosenv.2022.119446, 2023.

806 Yang, L., Luo, H., Yuan, Z., Zheng, J., Huang, Z., Li, C., Lin, X., Louie, P. K. K., Chen, D., and Bian, Y.:
807 Quantitative impacts of meteorology and precursor emission changes on the long-term trend of ambient ozone
808 over the Pearl River Delta, China, and implications for ozone control strategy, *Atmospheric Chemistry and Physics*,
809 19, 12901-12916, 10.5194/acp-19-12901-2019, 2019a.

810 Yang, W., Chen, H., Wang, W., Wu, J., Li, J., Wang, Z., Zheng, J., and Chen, D.: Modeling study of ozone source
811 apportionment over the Pearl River Delta in 2015, *Environmental Pollution*, 253, 393-402,
812 10.1016/j.envpol.2019.06.091, 2019b.

813 Yin, P., Chen, R., Wang, L., Meng, X., Liu, C., Niu, Y., Lin, Z., Liu, Y., Liu, J., Qi, J., You, J., Zhou, M., and Kan,
814 H.: Ambient Ozone Pollution and Daily Mortality: A Nationwide Study in 272 Chinese Cities, *Environmental*
815 *Health Perspectives*, 125, 10.1289/ehp1849, 2017.

816 Ying, Q., Zhang, J., Zhang, H., Hu, J., and Kleeman, M. J.: Atmospheric Age Distribution of Primary and
817 Secondary Inorganic Aerosols in a Polluted Atmosphere, *Environmental Science & Technology*, 55, 5668-5676,
818 10.1021/acs.est.0c07334, 2021.

819 Zeren, Y., Zhou, B., Zheng, Y., Jiang, F., Lyu, X., Xue, L., Wang, H., Liu, X., and Guo, H.: Does Ozone Pollution
820 Share the Same Formation Mechanisms in the Bay Areas of China?, *Environmental Science & Technology*, 56,
821 14326-14337, 10.1021/acs.est.2c05126, 2022.

822 Zhang, R. and Hanaoka, T.: Deployment of electric vehicles in China to meet the carbon neutral target by 2060:
823 Provincial disparities in energy systems, CO₂ emissions, and cost effectiveness, *Resources, Conservation and*
824 *Recycling*, 170, 10.1016/j.resconrec.2021.105622, 2021.

825 [Zhan, C., Xie, M., Huang, C., Liu, J., Wang, T., Xu, M., Ma, C., Yu, J., Jiao, Y., Li, M., Li, S., Zhuang, B., Zhao,](#)
826 [M., and Nie, D.: Ozone affected by a succession of four landfall typhoons in the Yangtze River Delta, China:](#)
827 [major processes and health impacts, *Atmospheric Chemistry and Physics*, 20, 13781-13799, 10.5194/acp-20-](#)
828 [13781-2020, 2020.](#)

829 Zheng, H., Kong, S., He, Y., Song, C., Cheng, Y., Yao, L., Chen, N., and Zhu, B.: Enhanced ozone pollution in the
830 summer of 2022 in China: The roles of meteorology and emission variations, *Atmospheric Environment*, 301,
831 10.1016/j.atmosenv.2023.119701, 2023.

832

Formatted: English (Hong Kong SAR)